Journal of Engineering Mathematics **31:** 119–130, 1997.

A WKB analysis of radical growth in the hydrogen-air mixing layer

ANTONIO L. SÁNCHEZ[1], AMABLE LIÑÁN[2] and FORMAN A. WILLIAMS[3]
[1]*Area de Mecánica de Fluidos, Escuela Politécnica Superior Universidad Carlos III de Madrid, 28911 Leganés, Spain*
[2]*Departamento de Motopropulsión y Termofluidodinámica, E. T. S. I. Aeronauticos, Universidad Politécnica de Madrid, 28040 Madrid, Spain*
[3]*Center for Energy and Combustion Research University of California San Diego, La Jolla, CA 92093-0411, USA*

Received: 7 May 1996; accepted in revised form 21 October 1996

Abstract. The chain-branching process leading to ignition in the hydrogen-air mixing layer is studied by application of a novel WKB-like method with a four-step reduced scheme adopted for the chemistry description. Attention is restricted to initial free-stream temperatures above the crossover temperature corresponding to the second explosion limit of H_2-O_2 mixtures, thereby causing three-body recombination reactions to be negligible in the ignition process. It is shown that the initiation reactions, responsible for the early radical buildup, cease being important when the radical mass fractions reach values of the order of the ratio of the characteristic branching time to the characteristic initiation time, a very small quantity at temperatures of practical interest. The autocatalytic character of the chain-branching reactions causes the radical concentrations to grow exponentially with downstream distance in the process that follows. It is shown that, because of the effect of radical diffusion, the radical growth rate is uniform across the mixing layer in the first approximation, with an exponent given by that of a premixed branching explosion evaluated at the location where the effective Damköhler number based on the flow velocity is maximum. This exponent, as well as the leading-order representation of the radical profiles, are easily obtained by the imposition of a bounded, nonoscillatory behavior on the solution.

Key words: chain branching, mixing layer, ignition, WKB

1. Introduction

The study of ignition in non-premixed reactive flows requires consideration of a number of complicating effects that do not emerge when addressing premixed combustion. Clarification of these effects can be aided by analysis of simplified flow-field models. Two such models are the counterflow and co-flow laminar mixing layers, which result in ignition problems with different mathematical characters [1, 2]. When a branching mechanism is involved, the ellipticity associated with the counterflow configuration causes the branch of ignited solutions to emerge as a bifurcation from the frozen state [3, 4]. In contrast, chain-branching ignition in co-flow mixing layers is a parabolic problem that leads to a continuous growth of the radical pool in a self-accelerating manner, observed in previous numerical studies [5, 6]. Although some analytical work on chain-branching ignition in the hydrogen-air mixing layer has been reported [7, 8], mixing-layer radical growth, in particular in relationship to the non-premixed character of the flow field, remains poorly understood and is addressed here.

It is helpful initially to recall the solution for the simple premixed chain-branching explosion [9]. Because of the autocatalytic nature of the process, with radical-production rates being linearly proportional to radical concentrations, the radical pool exhibits an exponential growth as time progresses, with an exponent proportional to the reaction-rate constant of the branching step. Similarly, chain-branching explosions in premixed, isovelocity, one-dimensional streams are characterized by an exponential increase of the radical pool with distance, linearly propor-

tional to the reaction-rate constant and inversely proportional to the flow velocity. Application of the same principle to the study of co-flow mixing layers encounters difficulties associated with the spatial variations of stoichiometric ratio, temperature and flow velocities that appear across the layer. Although one might expect the radical concentration to grow at each location with a rate proportional to the local effective Damköhler number based on the flow velocity, reactant concentration and temperature, this intuitive behavior soon breaks down because of the effect of diffusion. With diffusion neglected, as distance increases, the maximum radical concentration at the maximum local Damköhler number becomes exponentially large compared with radical concentrations elsewhere, and the profile develops a sharp peak. Diffusion of radicals to less populated regions then becomes more pronounced at this location, thus rapidly smoothing the peak. The solution that emerges in the presence of diffusion, obtained below by a WKB-like asymptotic technique, shows the following characteristics.

Diffusion prevents the radical profile from developing sharp peaks, and causes the exponential growth rate at leading order to be constant everywhere. The value of the growth rate, a quantity independent of radical diffusion in the first approximation, can be found as that of a premixed chain-branching explosion evaluated where the ratio of the convective residence time (proportional to the inverse of the local velocity) to the branching time is maximum. In obtaining this constant value, we must impose a non-oscillatory behavior on the radical profiles, determined already in the first approximation by a full balance between convection, diffusion and chemical production. The resultant profiles peak at the location of maximum local Damköhler number and decay exponentially to the sides. Analysis of the solution in the vicinity of the maximum, which is a turning point of the WKB expansion, yields the second-order correction to the growth rate as an eigenvalue in a linear eigenvalue problem.

Attention is restricted to hydrogen-air mixing layers with free-stream temperatures above the crossover temperature corresponding to the second explosion limit of H_2-O_2 mixtures [10]. Under those conditions, the effect of three-body recombination reactions is negligible, and the two streams mix and react initially without significant heat release, thereby giving rise to an approximately isothermal branched-chain explosion. In the early stages of the process, radical concentrations are very low, and the slow initiation steps control the process. Very soon the radical pool becomes large enough for the branching steps to take over, giving rise downstream to exponentially increasing radical concentrations with the previously described structure. This branching region ends where the radicals achieve their peak concentrations corresponding to partial equilibrium of the shuffle reactions, ushering in a region of radical recombination with significant heat release which leads to the development of a diffusion flame, a process not addressed in the present paper.

Four-step reduced chemistry with H and O as chain-branching species [4] will be employed. Description of the process of rapid radical growth will be obtained by means of an appropriate WKB method, involving exponential expansions for the radical concentrations in a series of decaying powers of the streamwise distance. In particular, the leading-order growth rate and radical profiles will be determined. A more complete analysis, including calculation of the second-order growth rate, will be performed for three-step chemistry with H atoms being the only chain-branching species not in steady state, and the results will be shown to compare well with those of numerical integrations of the full H-atom conservation equation.

2. Reduced kinetic mechanism and formulation

In high-temperature ignition the concentration of H_2O_2 remains negligibly small and the eight elementary steps $H_2+O_2\xrightarrow{0}OH+OH$, $H_2+O_2\xrightarrow{1}HO_2+H$, $H+O_2\xrightarrow{2}OH+O$, $H_2+O\xrightarrow{3}OH+H$, $H_2+OH\xrightarrow{4}H_2O+H$, $HO_2+H\xrightarrow{5}H_2+O_2$, $HO_2+H\xrightarrow{6}OH+OH$ and $H+O_2+M\xrightarrow{7}HO_2+M$ suffice to describe the chain-branching process in premixed [10] and non-premixed systems [4]. If the initial temperature is sufficiently above crossover, which is the case considered in the present study, then the rate corresponding to the reaction $H+O_2+M\xrightarrow{7}HO_2+M$ is negligible compared to that of the reaction $H+O_2\xrightarrow{2}OH+O$ and radical recombination can be neglected in the first approximation. Under those conditions, the concentration of hydroperoxyl radicals, whose production is then restricted to the slow initiation step $H_2+O_2\xrightarrow{1}HO_2+H$, remains negligibly small, and reactions $HO_2+H\xrightarrow{5}H_2+O_2$ and $HO_2+H\xrightarrow{6}OH+OH$ can be removed from the mechanism. Furthermore, since most of the heat released in hydrogen-oxygen combustion is associated with three-body radical recombinations, far above crossover the resultant branch-chained explosion becomes a nearly isothermal process.

An additional simplification follows from the assumption that the OH radical maintains steady state everywhere, an assumption valid for configurations which are not too fuel lean that was previously utilized in analyses of ignition in counterflow systems [4, 11]. The introduction of this steady-state assumption reduces the mechanism to the four-step description

$$3H_2+O_2\rightarrow 2H+2H_2O, \qquad H_2+O_2\rightarrow H+HO_2,$$

$$H_2+O_2\rightarrow O+H_2O, \qquad 2H_2+O_2\rightarrow 2H+H_2O,$$

with global rates given by $\omega_0, \omega_1, \omega_2$ and ω_3. Here, ω_j denotes the rate corresponding to the elementary step j. The reaction-rate constants corresponding to steps 0–3 are of the form $k_j = A_j T^{n_j}\exp[-E_j/(R^oT)]$, where R^o is the universal gas constant, Updated values of the different reaction-rate parameters in mol/cm^3, s^{-1}, K and cal/mol are [11] $A_0 = 1{\cdot}7\times10^{13}, A_1 = 13{\cdot}8\times10^{13}, A_2 = 3{\cdot}52\times10^{16}, A_3 = 5{\cdot}06\times10^{4}, n_0 = 0, n_1 = 0, n_2 = -0{\cdot}7, n_3 = 2{\cdot}67, E_0 = 47780, E_1 = 59607, E_2 = 17070$ and $E_3 = 6290$.

We consider a laminar mixing layer consisting of two parallel streams, one of hydrogen diluted with nitrogen and the other of air. In the formulation, x and y will be the coordinates in the streamwise and transverse directions, with u and v being their corresponding velocity components. The air and fuel streams occupy initially the upper $(y>0)$ and lower $(y<0)$ sides, merging at $x=0$ where mixing and reaction begin. The subscripts ∞ and $-\infty$ will denote free-stream conditions on the air and fuel sides, respectively. We shall assume, for simplicity, that density and transport properties are constant. For the flow considered, there exist self-similar solutions for the velocity field and for the frozen reactant concentrations and frozen temperature distribution, which are obtained by use of a similarity coordinate $\eta = [\rho u_\infty/(2\mu)]^{1/2}y/x^{1/2}$ and a nondimensional stream function $F(\eta)$, such that $u = u_\infty F'$ and $v = [\mu u_\infty/(2\rho x)]^{1/2}(\eta F' - F)$, where the prime denotes differentiation with respect to η and ρ and μ are the density and viscosity of the mixture [9]. With these new variables, the governing boundary-layer equations for the mixing layer with N different reactive species become

$$F''' + FF'' = 0, \tag{1}$$

$$2xF'\frac{\partial Y_i}{\partial x} - FY_i' - \frac{1}{S_i}Y_i'' = \frac{2x}{\rho u_\infty}w_i \tag{2}$$

$$2xF'\frac{\partial\theta}{\partial x} - F\theta' - \frac{1}{Pr}\theta'' = -\frac{2x}{c_pT_\infty\rho u_\infty}\sum_{i=1}^{N} h_i^o w_i, \tag{3}$$

where $\theta = (T - T_\infty)/T_\infty$ is an appropriate nondimensional temperature defined with respect to the air-side temperature, c_p is the specific heat at constant pressure of the mixture, $Pr = \mu c_p/\lambda$ is the Prandtl number and $Y_i, S_i = \mu/(\rho D_i), w_i$ and h_i^o are the mass fraction, Schmidt number, mass rate of production and enthalpy of formation of species i, respectively. The transport coefficients λ and D_i correspond to the thermal conductivity of the mixture and the binary diffusion coefficient of species i.

Equations (1)–(3) must be integrated subject to the boundary conditions $F' = 1, Y_i = Y_{i\infty}$ and $\theta = 0$ at $\eta = \infty, F' = \gamma = u_{-\infty}/u_\infty, Y_i = Y_{i-\infty}$ and $\theta = \theta_{-\infty} = (T_{-\infty} - T_\infty)/T_\infty$ at $\eta = -\infty$ and $F = 0$ at $\eta = 0$. In addition to the above boundary conditions, we must provide initial conditions for the integration of Equations (2) and (3) given by the uniform free-stream profiles $Y_i = Y_{i\infty}$ and $\theta = 0$ for $\eta > 0$ and $Y_i = Y_{i-\infty}$ and $\theta = \theta_{-\infty}$ for $\eta < 0$. Note that, with the simplifying assumptions introduced, Equation (1) is decoupled and can be integrated separately to yield the self-similar solution for the velocity profile.

Because of the autocatalytic exponential radical growth with distance that characterizes chain-branching ignition, the effect of reactant consumption is only important close to the ignition point at which the radical concentrations reach the values corresponding to partial equilibrium of the shuffle reactions. Also, in this high-temperature regime heat release is only significant downstream of this ignition point. Hence, the ignition distance can be determined in the first approximation by integration of the H-atom and O-atom conservation equations with the chemical terms evaluated with frozen reactant concentrations and frozen temperature θ_f. To write these equations, it is convenient to define normalized H-atom and O-atom mass fractions $y_{\mathrm{H}} = (4k_{2\infty})/(2k_{0\infty} + k_{1\infty})(Y_{\mathrm{H}}/Y_{\mathrm{H}_2-\infty})$ and $y_{\mathrm{O}} = (4k_{2\infty})/(2k_{0\infty} + k_{1\infty})(Y_{\mathrm{O}}/Y_{\mathrm{O}_2\infty})$, together with a new streamwise coordinate $\xi = (2\rho Y_{\mathrm{O}_2\infty}k_{2\infty})/(y_\infty W_{\mathrm{O}})x$ scaled with the characteristic air-side branching distance. With these new variables, the radical conservation equations with the Frank-Kamenetskii approximation adopted for the reaction-rate constants become

$$2\xi F'\frac{\partial y_{\mathrm{H}}}{\partial\xi} - Fy'_{\mathrm{H}} - \frac{1}{S_{\mathrm{H}}}y''_{\mathrm{H}} = \xi[\exp(\bar{\beta}\theta_f)y_{\mathrm{O}_2 f}y_{\mathrm{H}_2 f} + r\exp(\beta_3\theta_f)y_{\mathrm{H}_2 f}y_{\mathrm{O}}] \tag{4}$$

and

$$2\xi F'\frac{\partial y_{\mathrm{O}}}{\partial\xi} - Fy'_{\mathrm{O}} - \frac{1}{S_{\mathrm{O}}}y''_{\mathrm{O}} = \xi s[\exp(\beta_2\theta_f)y_{\mathrm{O}_2 f}y_{\mathrm{H}} - r\exp(\beta_3\theta_f)y_{\mathrm{H}_2 f}y_{\mathrm{O}}], \tag{5}$$

with boundary conditions $y_{\mathrm{H}} = y_{\mathrm{O}} = 0$ at $\xi = 0$ and at $\xi > 0, \eta = \pm\infty$. Here, $y_{\mathrm{O}2f}$ and $y_{\mathrm{H}_2 f}$ are the frozen reactant concentrations normalized with their free-stream values, $\beta_j = E_j/(R^oT_\infty)$ is the nondimensional activation energy of reaction $j, \bar{\beta}$ is an average of β_0 and $\beta_1, s = (W_{\mathrm{O}}Y_{\mathrm{H}_2-\infty})/(W_{\mathrm{H}_2}Y_{\mathrm{O}_2\infty})$ is an appropriate oxygen-to-fuel mass ratio, with W_i denoting the molecular weight of species $i (s = 8/0{\cdot}23$ for undiluted fuel with air), and $r = k_{3\infty}/k_{2\infty} \simeq 2{\cdot}9$ is the reaction-rate ratio corresponding to the controlling branching steps.

3. The chain-branching explosion

In the formulation employed, the ratio $(2k_{0\infty}+k_{1\infty})/k_{2\infty}$ is used as a scale for the radical mass fractions. This quantity, typically extremely small with values at $T_\infty = 1200$ and $T_\infty = 2000$

given approximately by $3{\cdot}6 \times 10^{-7}$ and 10^{-4}, is a measure of the characteristic radical mass fraction for which the rates of the initiation and branching steps are equal. Use of this scaling helps to expose the different characteristic regions that appear in the chain-branching explosion as mixing and reaction proceed.

In the early stages of the chain-branching process the rates of the branching reactions, which are proportional to the concentrations of radicals, are very small, and radical growth depends mainly on the initiation reactions. This initiation-controlled region corresponds to radical mass fractions smaller than the quantity $(2k_{0\infty} + k_{1\infty})/k_{2\infty}$ and, consequently, to values of y_{H} and y_{O} smaller than unity. Correspondingly, the streamwise extent of this region is such that $\xi \ll 1$, as can be seen from Equation (4). Observation of Equations (4) and (5) reveals that the initial growth of the radical pool is such that $y_{\mathrm{H}} \propto \xi$, whereas the mass fraction of O atoms, whose production is mainly controlled by step 2, remains smaller, with a streamwise variation given by $y_{\mathrm{O}} \propto \xi^2$. This initial region ends when the radical mass fractions reach small values of order $(2k_{0\infty} + k_{1\infty})/k_{2\infty}$. In the following intermediate region, which corresponds to values of y_{H}, y_{O} and ξ of order unity, all transport and chemical terms in (4) and (5) are equally important. The effect of initiation ceases being significant as the radical mass fractions increase to values large compared to $(2k_{0\infty} + k_{1\infty})/k_{2\infty}$. Further downstream, only branching steps must be retained in the mechanism to study the process of rapid radical growth that occurs. Since the values of the radical mass fractions corresponding to partial equilibrium of the shuffle reactions are typically of order unity, the values of y_{H} and y_{O} at the ignition point are large quantities of characteristic value $k_{2\infty}/(2k_{0\infty} + k_{1\infty})$. Correspondingly, the ignition point is located at a value of the streamwise coordinate ξ much larger than unity, and the asymptotic behavior of the solution for large values of ξ must be considered if a simplified expression for the ignition distance is to be obtained.

The linearity of (4) and (5) suggests that the solution to the homogeneous parabolic problem that results from removing the initiation term can be approximated for large values of ξ by exponential series of the WKB type [12] of the form $\exp\,[\xi \Sigma_{n=0}^{\infty} \xi^{-n/2} G_n(\eta)]$. In this approximation, we must choose the exponentially large terms in the expansions for y_{H} and y_{O} to be equal, so that the transport and chemical terms in Equations (4) and (5) can balance everywhere. Neglecting small terms of order $\xi^{-1/2}$ in the approximated series, we obtain

$$\frac{y_{\mathrm{H}}}{\phi_{\mathrm{H}}(\eta)} = \frac{y_{\mathrm{O}}}{\phi_{\mathrm{O}}(\eta)} = \exp[\xi G_0(\eta) + \xi^{1/2} G_1(\eta)]. \tag{6}$$

Introducing the above expressions into (4) and (5) and collecting terms of the same order in powers of ξ, we can solve the problem sequentially as follows.

At leading order, ξ^2, diffusion dominates, giving the single-term equation

$$G_0'^2 = 0. \tag{7}$$

This corresponds to the previously mentioned effect of diffusion. If G_0 were a function of η, then it would present a maximum at a certain location, where radical profiles would tend to grow faster in the limit of large streamwise distances. The associated large concentration gradients that would emerge in this region of rapid growth would readily enhance radical diffusion towards more diluted regions, resulting in a larger growth rate there. The overall effect of this equalizing mechanism is to cause the radical pool to grow in the first approximation with uniform exponential rate G_0, which will be determined below by carrying the analysis to a higher order.

The equation that emerges at the next order ($\xi^{3/2}$),

$$G_0' G_1' = 0, \tag{8}$$

is satisfied identically for any constant value of G_0, while the terms of order ξ yield the homogeneous linear system of equations

$$\begin{aligned} &[2F'G_0 - (S_{\mathrm{H}})^{-1} G_1'^2]\phi_{\mathrm{H}} - r\exp(\beta_3\theta_f) y_{\mathrm{H}_2 f}\phi_{\mathrm{O}} = 0, \\ &-s\exp(\beta_2\theta_f) y_{\mathrm{O}_2 f}\phi_{\mathrm{H}} + [2F'G_0 - (S_{\mathrm{O}})^{-1} G_1'^2 + rs\exp(\beta_3\theta_f) y_{\mathrm{H}_2 f}]\phi_{\mathrm{O}} = 0, \end{aligned} \tag{9}$$

which must satisfy the boundary conditions $\phi_{\mathrm{H}} = \phi_{\mathrm{O}} = 0$ at $\eta = \pm\infty$. Existence of nontrivial solutions to this problem requires that the determinant of the coefficient matrix associated with the above system of equations must vanish everywhere. This condition provides the quadratic equation for $G_1'^2$

$$\begin{aligned} &G_1'^4 - [2(S_{\mathrm{H}} + S_{\mathrm{O}})G_0F' + S_{\mathrm{O}} rs\exp(\beta_3\theta_f) y_{\mathrm{H}_2 f}]G_1'^2 \\ &\quad + 2S_{\mathrm{H}} S_{\mathrm{O}} G_0 F'[2G_0F' + rs\exp(\beta_3\theta_f) y_{\mathrm{H}_2 f}] \\ &\quad - S_{\mathrm{H}} S_{\mathrm{O}} rs\exp(\beta_2\theta_f)\exp(\beta_3\theta_f) y_{\mathrm{O}_2 f} y_{\mathrm{H}_2 f} = 0, \end{aligned} \tag{10}$$

which can easily be solved to yield two different solutions for $G_1'^2$. It can be shown that one of the resultant solutions never vanishes for any positive value of G_0, thereby giving two G_1 profiles monotonically increasing or decreasing with η. This behavior is not compatible with the boundary conditions $y_{\mathrm{H}} = y_{\mathrm{O}} = 0$ at $\eta = \pm\infty$ and, therefore, these two solutions must be disregarded. The number of locations where the other solution for $G_1'^2$ vanishes, which are turning points of the WKB expansion [12], depends on the value of G_0 as can be seen from Equation (10). If the value of G_0 is large enough, then no turning points appear, and the resulting solutions for G_1 would either increase or decrease monotonically with η, which is not acceptable as previously explained. For values of G_0 smaller than a critical value G_0^* the solution would exhibit two turning points, between which the resultant radical profiles would be oscillatory. It can be shown that the number of extrema of the profiles solutions to (4) and (5) remains constant as ξ increases. Since the initiation reaction causes the radical profiles to posses a single maximum in the initial stages of the chain-branching explosion, oscillatory behaviors cannot develop, thus preventing the existence of two turning points across the mixing layer. Therefore, the asymptotic solution that emerges must present a single turning point, a condition that determines uniquely the value of G_0^*. We calculated this value, as well as the location of the turning point η^*, from simultaneous solution of the equations

$$G_0^* F' = \tfrac{1}{4}\{rs\exp(\beta_3\theta_f) y_{\mathrm{H}_2 f}([4\exp(\beta_2\theta_f) y_{\mathrm{O}_2 f}/(rs\exp(\beta_3\theta_f) y_{\mathrm{H}_2 f}) + 1]^{1/2} - 1)\}, \tag{11}$$

$$G_0^* F'' = \tfrac{1}{4}\{rs\exp(\beta_3\theta_f) y_{\mathrm{H}_2 f}([4\exp(\beta_2\theta_f) y_{\mathrm{O}_2 f}/(rs\exp(\beta_3\theta_f) y_{\mathrm{H}_2 f}) + 1]^{1/2} - 1)\}', \tag{12}$$

obtained from (10) by imposing the merging to a single turning point. The corresponding value of the function $G_1'^2$ is positive everywhere except at η^*, where it presents a single zero. The boundary conditions at $\eta = \pm\infty$ indicate that we must choose the positive G_1' to describe the solution for $\eta < \eta^*$ and, similarly, the negative G_1' as $\eta \to \infty$, with transition between both solutions taking place at the turning point, where the radical profiles peak.

To clarify the physical significance of this result, we must notice that the left-hand side of (11) is inversely proportional to the local residence time of the flow, whereas its right-hand side, a function that exhibits a maximum at an intermediate position across the mixing layer and decays exponentially as the free-stream boundaries are approached, is inversely proportional to the local effective chemical time corresponding to the reaction mechanism considered. Therefore, imposing Equations (11) and (12) amounts to saying that the leading-order exponential growth rate G_0^*, which is constant across the mixing layer, corresponds to that of the maximum local effective Damköhler number based on the flow velocity, indicating that radical diffusion does not affect the chain-branching rate in the first approximation. Although this convection-controlled behavior of chain-branching processes in non-premixed mixing layers was previously pointed out by Treviño and Liñán [7], their conclusion arose from observation of numerical integrations of the conservation equations, rather than from a rigorous mathematical analysis as the one presented here.

The above analysis leading to (11) and (12) can be further clarified when we consider the evolution of the radical pool if radical diffusion were artificially removed from the system. In that case, radical growth would proceed independently at each location across the mixing layer. Determination of the radical-concentration evolution at each value of η would involve solution of the homogeneous system of equations given by (9) with the diffusion terms neglected, yielding a quadratic characteristic equation for G_0, containing only the last two terms in (10), which possesses a positive and a negative root. Whereas the positive root, given in Equation (11), corresponds to a growing solution that dominates the radical-growth process as the flow proceeds downstream, the negative root gives an exponentially decreasing contribution to the radical concentration which can be neglected to study the asymptotic behavior for large values of ξ, as it was done here in deriving (11) and (12), where negative values of G_0 were not considered. It is worth remarking that retaining this exponentially decreasing solution would be necessary to describe the transition of the solution from the initiation-controlled region to the region of autocatalytic exponential growth. Therefore, Equation (11) yields for each value of η the exponential radical-growth rate with downstream distance corresponding to a branched-chain explosion for a flow with velocity, temperature and composition evaluated at η. Combining this result with the condition that G_0^* must be maximum, which follows from Equation (12), we can conclude as before that, at leading order, the uniform exponential growth rate with downstream distance in the nonpremixed co-flow mixing layer is that of a premixed chain-branching explosion evaluated at the location across the mixing layer where the explosion distance is minimum.

Once Equations (11) and (12) are solved for G_0^* and η^*, we can integrate the function G_1' obtained from (10) to find the asymptotic form of the radical profiles. However, the maximum value, $G_1^* = G_1(\eta^*)$, of G_1 remains undetermined in the integration. We need to resolve the structure of the turning point in order to find this value as shown below. Although the explicit determination of the functions ϕ_{H} and ϕ_{O} requires that we carry the analysis to a higher order, solution to the homogeneous system given in (9) provides the ratio $\phi_{\mathrm{O}}/\phi_{\mathrm{H}}$.

4. WKB analysis with three-step simplified chemistry

Except for very dilute fuel feed, the previously defined oxygen-to-fuel mass ratio s takes very large values, causing the rates of production and consumption of O atoms to be much larger than the corresponding transport rates over most of the mixing layer, as can be seen from Equation (5). In this case, we can simplify the chemistry description further by assuming

that the O radicals are in steady state, an assumption that fails far into the air side, where the fuel concentration becomes too limited to maintain the O-atom consumption rate as explained elsewhere [4]. Introducing this assumption, we leave the H atom as the only chain-branching species not in steady state, thus reducing the chemistry to the three-step description $3H_2 + O_2 \rightarrow 2H + 2H_2O$, $H_2 + O_2 \rightarrow H + HO_2$ and $3H_2 + O_2 \rightarrow 2H + 2H_2O$, with global rates ω_0, ω_1 and ω_2. The problem then reduces to the integration of the radical conservation equation

$$2\xi F' \frac{\partial y_{\mathrm{H}}}{\partial \xi} - F y'_{\mathrm{H}} - \frac{1}{S_{\mathrm{H}}} y''_{\mathrm{H}} = \xi[\exp(\bar{\beta}\theta_f) y_{\mathrm{O}_2 f} y_{\mathrm{H}_2 f} + \exp(\beta_2 \theta_f) y_{\mathrm{O}_2 f} y_{\mathrm{H}}] \tag{13}$$

with the boundary conditions stated after Equation (5). As before, introducing the expression given in (6) into the above equation with the initiation term neglected gives $G'_0 = 0$ at leading order, while collecting terms of order ξ, we find

$$G'_1 = \pm S_{\mathrm{H}}^{1/2} [2F' G_0 - y_{\mathrm{O}_2 f} \exp(\beta_2 \theta_f)]^{1/2}. \tag{14}$$

The value of G_0^* and the turning-point location are now obtained by the solution of $2F' G_0^* = y_{\mathrm{O}_2 f} \exp(\beta_2 \theta_f)$ and $2F'' G_0^* = [y_{\mathrm{O}_2 f} \exp(\beta_2 \theta_f)]'$, which corresponds to the limiting form of (11) and (12) for large values of s. With the kinetic mechanism considered, the branching rate is independent of the H_2 concentration. The resultant local Damköhler number, *i.e.* the ratio $y_{\mathrm{o}_2 f} \exp(\beta_2 \theta_f)/F'$, is always maximum at $\eta = \infty$ for free-stream temperatures such that $\theta_{-\infty} \leqslant 0$. This results in turning points located at $\eta = \infty$, where the fuel concentration is infinitely small and the O-atom steady state fails. This behavior was analyzed elsewhere [7]. Hence, the validity of this simplified model is restricted to configurations with fuel-side temperatures sufficiently larger than the corresponding air-side temperatures to give maximum branching rates and turning points at finite locations across the mixing layer. Under those conditions, the kinetic mechanism holds in the region where the H-atom profile peaks, with the O-atom steady state breaking down far from this point, thereby introducing only relatively small inaccuracies in the results. It is worth pointing out that the one-step reduced scheme would also be adequate for the analysis of chain-branching ignition in wakes, for which velocities are minimum in the center region and become larger as $\eta \rightarrow \pm\infty$. In such flows the local residence time decreases as we move away from the center region, and ignition always occurs at a finite location where the local effective Damköhler number is maximum.

The asymptotic solution described here holds away from the turning point, but breaks down in the vicinity of $\eta = \eta^*$, where the H-atom mass fraction must evolve from an exponentially growing solution as $\eta \rightarrow \eta^*$ to an exponentially decaying profile for $\eta > \eta^*$. The analysis of this transition region, which is briefly sketched below, provides the second-order correction to the growth rate G_1^*. Introducing a stretched coordinate $\zeta = (4aS_{\mathrm{H}})^{1/4}(\eta - \eta^*)\xi^{1/4}$ and a new function $\psi(\zeta)$ given by $y_{\mathrm{H}} = \psi(\zeta) \exp[\xi G_0^* + \xi^{1/2} G_1^*]$ into Equation (13), we obtain the parabolic cylinder equation (13)

$$\frac{\partial^2 \psi}{\partial \zeta^2} - \left(\frac{\zeta^2}{4} + \Lambda \right) \psi = 0, \tag{15}$$

where $a = [2F' G_{\mathrm{O}}^* - y_{\mathrm{O}_2 f} \exp(\beta_2 \theta_f)]''/2$ and $\Lambda = (S_{\mathrm{H}}/a)^{1/2} F' G_1^*/2$, with the functions F' and $[2F' G_{\mathrm{O}}^* - y_{\mathrm{O}_2 \mathrm{f}} \exp(\beta_2 \theta_f)]''$ being evaluated at $\eta = \eta^*$. The solution to Equation (15)

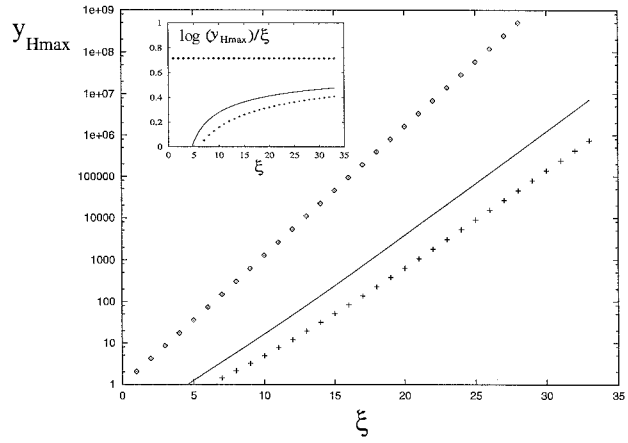

Figure 1. Comparison of the evolution of $y_{\mathrm{H\,max}}$ with ξ for $\theta_{-\infty} = 0{\cdot}3$ obtained from integration of Equation (13) (lines) with the leading-order $y_{\mathrm{H\,max}} = \exp(G_0^*\xi)$ (rhomboids) and second-order $y_{\mathrm{H\,max}} = \exp(G_0^*\xi + G_1^*\xi^{1/2})$ (crosses) predictions of the asymptotic analysis; the inset shows the same comparison for $\log(y_{\mathrm{H\,max}})/\xi$.

must be non-negative and decay exponentially to zero as $\zeta \to \pm\infty$ to match with the H-atom profiles corresponding to the WKB expansion. This behavior that can only be achieved for

$$\Lambda = -\tfrac{1}{2}, \tag{16}$$

giving an associated eigenfunction

$$\psi = \exp(-\zeta^2/4). \tag{17}$$

Therefore, Equation (16), together with the definition of the parameter Λ, determines uniquely the negative value of G_1^* once the location of the turning point η^* has been obtained. This negative value reflects the influence of radical diffusion on the branching process, causing the maximum radical concentration to increase at a smaller rate, which is an effect that is not seen in the leading-order solution. It must be noticed that, to discriminate the solution $\Lambda = -1/2$ from the discrete set of eigenvalues that satisfy (15) with boundary conditions $\psi(\pm\infty) = 0$, we must impose a nonnegativity constraint on the solution. This constraint is associated with the absence of oscillatory radical profiles, a criterion that is also used at leading order to determine the value of G_0^*. Clearly, the imposition of a nonoscillatory behavior is a key part of the asymptotic solution presented here, providing consistency to the method and enabling the analysis to be extended to an arbitrarily high order.

As an example, we compare in Figure 1 the leading-order $y_{\mathrm{H\,max}} = \exp(G_0^*\xi)$ and second-order $y_{\mathrm{H\,max}} = \exp(G_0^*\xi + G_1^*\xi^{1/2})$ asymptotic predictions for $\theta_{-\infty} = 0{\cdot}3$ and a free-stream velocity ratio $\gamma = 1$ with the results obtained by integration of (13) with $\bar{\beta} = 0$. Included in an inset is also the comparison of the numerical value of $\log(y_{\mathrm{H\,max}})/\xi$ with the first-order and second-order asymptotic predictions G_0^* and $G_0^* + G_1^*\xi^{-1/2}$. In this isovelocity case the turning point is located where the function $y_{\mathrm{O}_2 f}\exp(\beta_2\theta_f)$ exhibits a maximum. Choosing $Pr = 0{\cdot}74$, $S_{\mathrm{O}_2} = 0{\cdot}74$ and $\beta_2 = 7$, we find a maximum value $y_{\mathrm{O}_2 f}\exp(\beta_2\theta_f) \simeq 1{\cdot}43$ located at $\eta^* \simeq -0{\cdot}07$, with a corresponding leading-order growth rate $G_0^* \simeq 0{\cdot}715$. The second-order growth rate $G_1^* \simeq -1{\cdot}7571$ is then determined from the curvature of the $y_{\mathrm{O}_2 f}\exp(\beta_2\theta_f)$ profile at $\eta = \eta^*$ with $S_{\mathrm{H}} = 0{\cdot}12$. As can be seen, the effect of radical diffusion on the chain-branching

rate, which is present in the second-order asymptotic prediction $y_{\mathrm{H}\,\max} = \exp(G_0^*\xi + G_1^*\xi^{1/2})$ through the negative value of G_1^*, is non-negligible if an accurate prediction of the ignition distance is to be obtained. Although an extension of the asymptotic analysis to a higher order would certainly improve the agreement with the results of the numerical integrations, the second-order approximation presented here already gives accuracies of ignition distances better than 10%, as can be seen in the figure.

5. Discussion and conclusions

The asymptotic analysis of the ignition process in laminar mixing layers presented above is based on the fact that the characteristic reaction time of the chain-branching reactions is very small compared with that of the initiation reactions, so that the latter only play a significant role when the mass fraction of the radicals is very small, namely of the order of the ratio of the reaction times. The main exponential growth of the radical mass fraction is due to the chain-branching reactions. The analysis shows that the mass fraction of H in the long ignition stage is given by the expression

$$\frac{Y_{\mathrm{H}}}{Y_{\mathrm{H_2}-\infty}} = \frac{2k_{0\infty} + k_{1\infty}}{4k_{2\infty}}\phi_{\mathrm{H}} \exp\left[\xi G_0^* + \xi^{1/2}\left(G_1^* + \int_{\eta^*}^{\eta} G_1' \,\mathrm{d}\eta\right)\right], \tag{18}$$

where $\xi = (2\rho Y_{\mathrm{O_2}\infty}k_{2\infty})/(u_\infty W_{\mathrm{O}})x$ and $G_0^*, G_1^*, G_1'(\eta)$ and ϕ_{H} are of order unity. The values of G_0^* and $G_1'(\eta)$, providing the leading-order representation for large ξ of the peak radical concentration and concentration profiles, are easily determined in terms of the frozen concentration and temperature profiles in the mixing layer.

The linear chain-branching ignition stage ends at a streamwise location ξ_{I} such that $Y_{\mathrm{H}}/Y_{\mathrm{H_2}-\infty}$ is of order unity. This ξ_{I} is given in the first approximation by the relation.

$$\xi_{\mathrm{I}} = \frac{\log[4k_{2\infty}/(2k_{0\infty} + k_{1\infty})]}{G_0^*}, \tag{19}$$

obtained from (18). The constant G_0^* is the maximum value of the local effective Damköhler number, represented by the right-hand side of (11) divided by the local flow velocity F'. Notice that if errors of order $\xi_{\mathrm{I}}^{1/2}$ are accepted in the determination of the large value ξ_{I} of the ignition-delay length, this length corresponds to the minimum delay length obtained, with the effect of radical diffusion neglected, across the chemically frozen mixing layer. The effects of conduction and diffusion enter obviously in the determination of the self-similar temperature and reactant concentration profiles.

We have seen that the computation of ξ_{I} with errors of order unity, which correspond to small relative errors of order ξ_{I}^{-1}, requires resolving the structure of the turning point where the radical profiles peak. Such an analysis is performed here for three-step reduced chemistry. This is a simplified scheme whose validity is restricted to configurations with fuel-side temperatures larger than the corresponding air-side temperatures. Solution of the turning-point structure that emerges when four-step reduced chemistry is employed would be necessary for obtaining accurate predictions of ignition distances in applications in which cold hydrogen is injected into a hot stream of air.

The analysis presented here can also be applied to the study of ignition events in mixing layers when wake effects are significant. In general, when two parallel streams merge at the end of a separating plate, there exists a momentum-deficit region in the vicinity of the trailing edge

where a longer residence time is available for chemical reactions to occur. The importance of the wake effect in the overall chain-branching process depends on the relative values of the characteristic branching time and characteristic residence time associated with this region. If attention is restricted to the study of self-similar regions such as the Goldstein [14] and Rott-Hakkinen [15] regions, then the necessary radical-growth analysis would be analogous to the one presented here. It can be anticipated that, since the wake velocity increases with the one-third power of the streamwise distance, the radical mass fractions in these regions would be proportional to $\exp(\xi^{2/3} G_0^*)$, where ξ is an appropriate nondimensional streamwise distance and G_0^* is the maximum effective Damköhler number across the wake. In determining the value of G_0^* one must account for the large velocity variations that exist within the wake.

The present study contributes new information of two types concerning high-temperature ignition in laminar hydrogen-air mixing layers relevant to conditions like those encountered in supersonic-combustion applications. The results improve knowledge of the physics of the process by showing how radical diffusion introduces uniformity of radical-pool growth across the mixing layer in the first approximation, leading to ignition distances independent of radical diffusion coefficients and proportional to the flow velocity. The analysis also shows for the first time how mathematical methods based on the WKB approach can be applied to such problems through suppression of oscillatory components.

Acknowledgements

The work of A. L. Sánchez was supported by the Spanish DGICYT under Contract No. PB95-0280, the work of A. Liñán was supported by the Spanish CICYT under Contract No. PB94-0400 and by INTA under Contract No. INTA 4070-0036/1995 and the work of F. A. Williams was supported by the National Science Foundation through Grant No. CTS 95-26410.

References

1. A. Liñán, The asymptotic structure of counterflow diffusion flames for large activation energies. *Acta Astronautica* 1 (1974) 1007–1039.
2. A. Liñán and A. Crespo, An asymptotic analysis of unsteady diffusion flames for large activation energies. *Combust. Sci. Tech.* 14 (1976) 95–117.
3. A. L. Sánchez, A. Liñán and F. A. Williams, A bifurcation analysis of high-temperature ignition of H_2-O_2 diffusion flames. *Twenty-Fifth Symposium (International) on Combustion.* The Combustion Institute, Pittsburgh, PA (1994) 1529–1537.
4. A. L. Sánchez, G. Balakrishnan, A. Liñán and F. A. Williams, Relationships between bifurcation and numerical analysis for ignition of hydrogen-air diffusion flames. *Combust. Flame* 105 (1996) 569–590.
5. L. F. Figueira Da Silva, B. Deshaies and M. Champion, Some specific aspects of combustion in supersonic H_2-air laminar mixing layers. *Combust. Sci. Tech.* 89 (1993) 317–333.
6. Y. Ju and T. Niioka, Reduced kinetic mechanism of ignition for nonpremixed hydrogen/air in a supersonic mixing layer. *Combust. Flame* 99 (1994) 240–246.
7. C. Treviño and A. Liñán, Mixing layer ignition of hydrogen. *Combust. Flame* 103 (1995) 129–141.
8. H. G. Im, S. R. Lee and C. K. Law, Ignition in the supersonic hydrogen/air mixing layer with reduced reaction mechanisms. *J. Fluid Mech.* accepted for publication (1995).
9. F. A. Williams, *Combustion Theory.* Menlo Park (CA): Benjamin Cummings (1985) 680 pp.
10. C. Treviño, Ignition phenomena in H_2-O_2 mixtures. *Progress in Astronautics and Aeronautics, AIAA* 131 (1991) 19-43.
11. G. Balakrishnan, M. D. Smooke and F. A. Williams, A numerical investigation of extinction and ignition limits in laminar nonpremixed counterflowing hydrogen-air streams for both elementary and reduced chemistry. *Combust. Flame* 102 (1995) 329–340.
12. C. M. Bender and S, Orszag, *Advanced Mathematical Methods for Scientists and Engineers*. New York: McGraw Hill (1978) 593 pp.

13. M. Abramowitz and A. Stegun, *Handbook of Mathematical Functions.* New York: Dover (1965) 1046 pp.
14. S. Goldstein, Concerning some solutions of the boundary layer equations in hydrodynamics. *Proc. Cambridge Phil. Soc.* 26 (1930) 1–30.
15. N. Rott and R. J. Hakkinen, Similar solutions for merging shear flows. *J. Aerospace Sci.* 29 (1962) 1134–1135.